

The impact of calcium sulfate and inert solids accumulation in post-combustion calcium looping systems

M. Elena Diego ^{*}, Borja Arias, Mónica Alonso, J. Carlos Abanades

Spanish Research Council, INCAR-CSIC, C/Francisco Pintado Fe, 26, 33011 Oviedo, Spain

HIGHLIGHTS

- The effects of sulfur and the accumulation of inerts are quantitatively discussed.
- Mass and energy balances were solved together with an updated carbonator model.
- It was found that the main impact on CaL performance is due to the sulfur inlet.
- A minimum purge is required even when an effective reactivating step is carried out.

ARTICLE INFO

Article history:

Received 15 October 2012

Received in revised form 15 November 2012

Accepted 19 November 2012

Available online 5 December 2012

Keywords:

CO₂ capture
Calcium looping
Coal combustion
Sulfation
Carbonation

ABSTRACT

Postcombustion CO₂ capture by calcium looping (CaL) is being rapidly developed for coal combustion applications. This work discusses the impact of the accumulation of CaSO₄ and other inert solids on CO₂ capture efficiency and the overall CaL process performance. Several process configurations are considered, and the mass and energy balances and an updated carbonator reactor model are solved for each configuration. The minimum fresh sorbent requirements for sustaining a certain level of CO₂ capture efficiency are quantified as well as the effects of an increase in the make-up flow. It was found that the main effect on the CaL process is produced by the sulfur present in the coal fed to the calciner and in the flue gas entering the carbonator. For a typical set of operating conditions it was calculated that the deactivating effect caused by an increase of 0.5% in the sulfur content with respect to a reference coal (low ash content) fed to the calciner is similar to the effect caused by the accumulation of inerts when using a coal with 15% more ash.

© 2012 Elsevier Ltd. All rights reserved.

1. Introduction

CO₂ capture and storage (CCS) has emerged as a suitable option for reducing CO₂ emissions from large stationary sources such as coal power plants [1]. Nowadays there are mature CO₂ capture technologies that could be commercially deployed if there are reasonable incentives due to carbon prices [1]. In order to reduce the costs associated with CO₂ capture, a number of new technologies are also emerging. One of the most promising processes is post-combustion Ca-looping (CaL), which has experienced a rapid scale up in the last few years. It has already been tested in small facilities (10s kW_{th}) operating in full continuous mode [2,3] and has currently reached the experimental testing phase in a 1.7 MW_{th} pilot plant in La Pereda – Spain [4,5], a 200 kW_{th} facility at IFK – Stuttgart [6,7] and a 1 MW_{th} pilot plant at ETS in Darmstadt [8,9].

^{*} Corresponding author. Tel.: +34 985119090; fax: +34 985 297662.

E-mail address: marlen@incarcscic.es (M.E. Diego).

Postcombustion CaL was first proposed by Shimizu et al. [10], and is based on the use of lime as a sorbent to capture CO₂ by means of carbonation/calcination cycles. The most suitable configuration for the application of CaL on a large scale involves the use of two interconnected circulating fluidized bed (CFB) reactors (carbonator and calciner as shown in Fig. 1). In this process, the flue gas generated in the power plant is directed to a carbonator, where CO₂ reacts at temperatures between 600 and 700 °C with a stream of CaO particles. As a result, CaCO₃ is formed and a CO₂ depleted gas leaves the carbonator. The partially carbonated solid stream enters the calciner together with a continuous make-up flow of limestone fed to this reactor to compensate for the decay of the CO₂ capture capacity of the sorbent with the number of carbonation/calcination cycles. In the calciner coal burns under oxy-fired conditions [10] to attain the temperatures required to convert both the CaCO₃ from the carbonator and the fresh sorbent back to CaO (around 900 °C). Although the heat demand in this reactor (coal and O₂) is high [10,11], the overall energy penalty of the CaL process is low [10,12–19], since energy can be recovered from

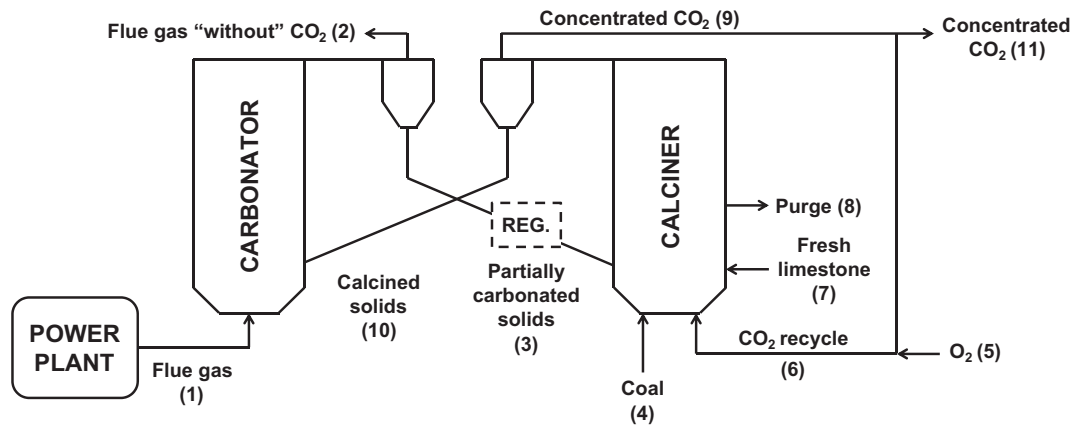


Fig. 1. General scheme of the CaL process for the three studied configurations. Dotted line indicates a possible location for the sorbent regenerator (REG.) in Configuration 3.

high-quality heat sources (the solids streams between reactors, the carbonator and the high temperature gases abandoning the reactors).

As a consequence of the nature of the CaL process, these systems have a continuous input of inert solids, mainly due to the coal fed into the circulating fluidized bed calciner but also because of the SO_2 in the flue gas entering the circulating fluidized bed carbonator. The SO_2 tends to react with the CaO present in both reactors of the system and forms CaSO_4 . In order to prevent the accumulation of inerts in the system, solids should be purged from the calciner, which will contain mainly CaO , CaSO_4 and ashes. The flow rate of the solids purge is defined from a mass balance of the inerts fed to the process and the fresh limestone added to the calciner. The ratio between these two variables also determines the composition of the total inventory of solids in the system, which is known to affect the performance of the calcium looping process in terms of CO_2 capture efficiency and heat requirements in the calciner [11,20,21]. Some previous works give an overall view of the CaL process by formulating the mass and energy balances of the whole system, and they analyze the performance of CaL under certain operating conditions, such as different make-up flows of limestone or different solids circulating rates between reactors [11,21], even in the presence of sulfur [12,20]. However, these studies do not analyze the influence of ashes and the formation of CaSO_4 on CO_2 capture efficiency from a carbonator reactor point of view. This is a critical relationship to be quantified in the system. For a certain set of operating conditions, the solids inventory in the circulating fluidized bed carbonator will be fixed, and an increase in the concentration of inert solids in the system will translate into a low inventory of active Ca inside the reactor, thereby reducing the CO_2 capture efficiency. The aim of this work therefore is to quantitatively discuss these effects by analyzing several scenarios in relation to different power plant and CO_2 capture configurations. For this purpose, mass and energy balances were solved together with an updated carbonator reactor model, allowing us to calculate the CO_2 capture efficiency for each scenario. This simulation exercise provided useful information to determine the minimum make-up flow of limestone required to sustain a certain level of CO_2 capture efficiency as a function of the quality of the coal fed to the calciner and the SO_2 content in the flue gas entering the carbonator reactor from the power plant.

2. Methodology for process simulation

The process configurations analyzed in this work follow the general scheme depicted in Fig. 1, in which the flue gas coming from the power plant is fed into the carbonator of the CaL facility.

Table 1

Outline of the process configurations used in this work.

Process configuration	Power plant	Sorbent reactivation
1	PC	No
2	CFBC	No
3	CFBC	Yes

Table 1 summarizes the different configurations of the process, depending on the type of power plant emitting flue gases, the availability of SO_2 capture from the flue gas (with a flue gas desulfurization (FGD) unit in the pulverized coal (PC) power plant or an in situ SO_2 capture in the circulating fluidized bed combustion (CFBC) power plant) or the presence of a reactivation process.

Configuration 1 consists of a PC power plant that uses low sulfur fuel with no flue gas desulfurization unit. Some previous works study the effect of SO_2 on the sorbent activity in postcombustion CaL [22–26]. They have shown that SO_2 accelerates the decrease in CO_2 carrying capacity during cycling. Therefore, some authors [23] have highlighted the need for desulfurization of the flue gas entering the carbonator. However, the possibility of using the CaL process as a CO_2 – SO_2 co-capture system translates into capital cost savings that may compensate for the additional limestone make-up requirements.

Configuration 2 is a CFBC power plant fitted with a CaL facility. High-efficient SO_2 capture (typically 90%) is assumed at the interior of the combustion chamber of the CFBC. For the purpose of this work, a similar PC + FGD + CaL configuration would give almost identical results to those obtained for this CFBC case. The only difference in favor of a CFBC power plant is that the purged material from the calciner can be used inside the CFBC as a sorbent to capture SO_2 from the flue gases.

Configuration 3 shows a similar scheme to that of Configuration 2, different only in that it incorporates a regenerator in the process. This reactivation step could be one of hydration [26–34], recarbonation [35] or any other means to increase the average activity of the circulating material or a fraction of such a solid stream. In order for the simulation to embrace any sorbent reactivation strategy no specific procedure to regenerate the solids is specified. The impact of the reactivation step is only considered through the increase in the average carrying capacity of the circulating material.

Mass and energy balances were solved for each configuration using an updated version of the carbonator model proposed by Alonso et al. [36]. This model assumes that the carbonator behaves as a continuous stirred tank reactor (CSTR) for the solids, so that the conversion of the particles is based on their residence time

distribution, whereas the carbonator performs as a plug flow reactor (PFR) for the gas phase. In this work the average reaction rate (r_{ave}) is expressed as [3]

$$r_{ave} = k_{SB} \phi f_a N_{Ca} X_{ave} (v_{CO_2} - v_e) \quad (1)$$

where $k_{SB} \phi$ is the apparent reaction rate constant, f_a is the active fraction of particles, N_{Ca} is the total inventory of Ca moles inside the carbonator, X_{ave} is the maximum average conversion of the solids, v_{CO_2} is the volume fraction of CO_2 and v_e is that in equilibrium conditions.

The fraction of particles that are active and able to react with CO_2 are those which have been in the carbonator for a shorter time than that required to achieve their maximum carbonate conversion, t^* [36]. Therefore, f_a is formulated in accordance with the CSTR residence time distribution [36]

$$f_a = \left(1 - \exp\left(\frac{-t^*}{N_{Ca}/F_R}\right) \right) \quad (2)$$

where F_R is the calcium looping rate between the reactors and t^* can be calculated from Eq. (3) [3,36]

$$t^* = \frac{X_{ave}}{(dX/dt)_{reactor}} = \frac{X_{ave}}{k_{SB} \phi X_{ave} (v_{CO_2} - v_e)} \quad (3)$$

The maximum average carbonation conversion of lime particles can be obtained from the expression proposed by Rodríguez et al. [37], assuming total calcination conversion. This equation takes into account the fact that the carbonation reaction may not be completed each time that a particle leaves the carbonator,

$$X_{ave} = \frac{a_1 f_1^2 F_0}{F_0 + F_R f_{carb} (1 - f_1)} + \frac{a_2 f_2^2 F_0}{F_0 + F_R f_{carb} (1 - f_2)} + b \quad (4)$$

In Eq. (4) F_0 represents the make-up flow of fresh limestone and a_1, f_1, a_2, f_2 and b are sorbent fitting constants of the X_N vs. N equation proposed by Li et al. [21]. f_{carb} stands for the extent of carbonation of the particles and can be obtained from the following expression [36]

$$f_{carb} = \frac{X_{carb}}{X_{ave}} = \frac{f_a}{\ln(1/(1 - f_a))} \quad (5)$$

The previous X_{ave} expression only considers the decay in the CO_2 capture capacity of lime resulting from the number of carbonation and calcination cycles. As was mentioned above, the impact of the SO_2 on the activity of the sorbent is difficult to quantify in a large scale system. A conservative assumption [12] can be made by assuming that sulfur reacts only with the active fraction of the sorbent, so that the effective maximum average conversion of the solids, $X_{ave,e}$, is obtained through the following expression,

$$X_{ave,e} = X_{ave} - X_{sulf} \quad (6)$$

In this equation X_{sulf} is the fraction of the fresh limestone that reacts with the sulfur that enters into the system with the flue gas and the coal burnt in the calciner, F_S [12]

$$X_{sulf} = \frac{F_S}{F_0} \quad (7)$$

Eqs. (4) and (6) do not directly reflect the positive impact of a potential sorbent reactivation stage (dotted box in Fig. 1). As discussed below, this will be taken into account when selecting the sorbent performance parameters (a_1, a_2, f_1, f_2 and b implicit in the equation proposed by Li et al. [21] and used to obtain Eq. (6)) in Configuration 3 reported in Table 1.

Finally, the last term of the reaction rate expression (Eq. (1)) is the average of the difference between the CO_2 volume fraction in the carbonator and that in equilibrium conditions, which is obtained through Eq. (8) [36]

$$\overline{v_{CO_2}} - v_e = \frac{E_{carb}}{\left[-\frac{v_0}{(v_0 v_e - v_0)} E_{carb} + \left(\frac{(v_0 v_e - v_0) + (v_0 - v_e) v_0}{(v_0 v_e - v_0)^2} \right) \ln \left(\frac{(v_0 - v_e) + (v_0 v_e - v_0) E_{carb}}{(v_0 - v_e)} \right) \right]} \quad (8)$$

In this expression E_{carb} symbolizes the CO_2 capture efficiency and v_0 is the CO_2 volume fraction at the carbonator inlet.

Taking into account all previous considerations, the carbon mass balance in the solids phase can be expressed as [36]

$$E_{carb} = \frac{F_R}{F_{CO_2}} X_{ave} \frac{f_a}{\ln(1/(1 - f_a))} \quad (9)$$

where F_{CO_2} is the CO_2 molar flow that enters the carbonator.

Moreover, the carbon mass balance formulated for the gas phase at the carbonator exit is given by the following equation,

$$\frac{F_{CO_2} PM_{Ca}}{W_{Ca} f_a k_{SB} \phi X_{ave}} \left[-\frac{v_0}{(v_0 v_e - v_0)} E_{carb} + \frac{v_0 (v_0 - 1)}{(v_0 v_e - v_0)^2} \ln \left(\frac{(v_0 - v_e) + (v_0 v_e - v_0) E_{carb}}{(v_0 - v_e)} \right) \right] = 1 \quad (10)$$

where PM_{Ca} and W_{Ca} are the average molecular weight and the inventory of Ca compounds, respectively.

To solve the previous equations, we have defined the following input variables: the power plant capacity, the composition of the coals used in the boiler and the calciner, the inlet gas velocity in the carbonator and its total inventory, the kinetic and sorbent decay constants, the total solids circulation between reactors, the make-up flow of limestone and the oxygen content and temperature of the recycled gas stream that enters into the calciner. After the simultaneous formulation of the energy and mass balances, together with the Eqs. (5), (9), and (10) of the carbonator model, we can calculate the fraction of active particles, their maximum CO_2 carrying capacity and carbonation conversion, the calcium looping rate between reactors, the coal and O_2 required in the calciner, and CO_2 capture efficiency in the carbonator.

3. Results and discussion

In order to analyze the relationship between CO_2 capture efficiency and the input of ashes and SO_2 to the CaL system for the three configurations of Table 1, a common set of boundary conditions was defined. A power plant capacity of 1000 MW_{th} was fixed for all the configurations, so that the CO_2 molar flow and the volume fraction entering the carbonator could be calculated. The chosen operating temperatures were 650 °C and 920 °C for the carbonator and calciner respectively. All reactors are assumed to operate under similar hydrodynamic conditions. For this purpose, the carbonator cross sectional area was calculated for all scenarios to maintain an inlet gas velocity in this reactor of 5 m/s. In addition, the total inventory of solids in the carbonator was set at 1000 kg/m² (including ashes and calcium sulfate). This inventory is assumed to be independent of the gas velocity in the carbonator and the solid circulation rate or the calcium ratio to the carbonator. This assumption only makes sense if modest changes are accepted in these variables and the possibility of an additional internal recycle of solids is considered in the scheme of Fig. 1 to decouple the solids inventory in the carbonator from the solids circulation between the reactors [38,39]. The F_0/F_{CO_2} ratio was fixed at 0.1 for all configurations and no losses of lime due to attrition were considered for the mass balances, as the attrition effects are known to be closely related to the first calcination step [40] (so that the material subjected to attrition is mainly the make-up flow fed to the system), and they can be compensated for by introducing a higher make-up flow of limestone. For this comparison exercise, we have assumed a total external solids circulation rate to the calciner of 5 kg/m²s which should be high enough to give high active

space times [3] to ensure high CO₂ capture efficiencies and reasonable heat requirements in the calciner of a CaL system [11]. The apparent reaction rate constant of active particles in the carbonator was taken as 0.43 s⁻¹ [3]. The SO₂ capture efficiency for both the carbonator and the calciner is assumed as 90% for each step. However, as a fraction of the gases leaving the calciner is recycled to this reactor, the overall calciner SO₂ capture efficiency increases.

The composition of the coal fed to the PC and CFB combustors is 68.0% C, 4.0% H, 1.0% S, 8.0% O, 8.0% H₂O, 1.0% N, 10.0% Ash (LHV: 28.0 MJ/kg). However, the CFB calciner requires a high quality coal in order to reduce the energy demand in the CaL facility [11] (74.0% C, 4.0% H, 0.5% S, 8.0% O, 8.0% H₂O, 0.5% N, 5.0% Ash (LHV: 30.0 MJ/kg)).

The amount of coal fed to the calciner is calculated by means of the energy balance. Coal is assumed to be burnt in the calciner with an oxidizing mixture containing 30%v O₂. The sulfur contained in the coal is mainly converted to calcium sulfate, as the CFB calciner is assumed to operate with a SO₂ capture efficiency of 90% for each step. The split between fly and bottom ashes from the coal (the latter are the only fraction that accumulates in the CaL system) was considered to be 50%. In addition, the flue gas coming from the power plant is assumed to be free of ashes.

Values of $a_1 = 0.1045$, $f_1 = 0.9822$, $a_2 = 0.7786$, $f_2 = 0.7905$ and $b = 0.07709$ were used as the fitting parameters of Eq. (4) to calculate X_{ave} [37]. These parameters are fully consistent with the data reported by Grasa et al. [41], which can be expressed through Eq. (4) to make easier to estimate X_{ave} under different conditions. Eq. (4) was also used to calculate X_{ave} for the reactivation step, but in this case the parameters were adjusted to achieve a different residual conversion of the sorbent. For Configuration 3, the fitting constants in Eq. (4) are: $a_1 = 0.1288$, $f_1 = 0.9744$, $a_2 = 0.7248$, $f_2 = 0.7730$ and $b = 0.1666$. This corresponds to a residual sorbent conversion (X_r) of around 0.16, which is equal to that obtained experimentally through recarbonation [35] (see Fig. 2). Nevertheless, similar or even higher levels of sorbent reactivation can be attained by using other strategies, such as hydration [26–34] or other options which are also being studied to improve the CO₂ capture capacity of lime [42,43]. It should be also mentioned that the previous fitting parameters derive from thermogravimetric studies done in the absence of steam, which may enhance the activity of the sorbent [44,45]. Fig. 2 shows the adjustment of Eq. (4) (with the new fitting constants) to the experimental values obtained through recarbonation [35]. The curve for the case where there was no reactivation is also depicted.

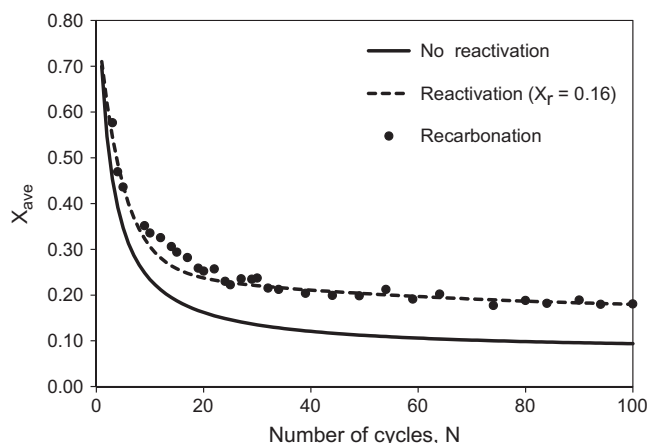


Fig. 2. X_{ave} curves for no reactivation and reactivation up to $X_r = 0.16$, and experimental results obtained by recarbonation [35].

Table 2

Results from the mass and energy balances for the configurations of Table 1.

Process configuration	E_{carb}	$X_{ave,e}$	X_{carb}	X_{sulf}
1	0.50	0.080	0.075	0.079
2	0.80	0.124	0.114	0.034
3	0.93	0.235	0.135	0.036

The mass and energy balances were solved for the central set of operating conditions for each configuration of Table 1, and the results are shown in detail in Tables 2–4.

As expected, CO₂ capture efficiency is significantly lower in Configuration 1 (see Table 2). In this case, the high SO₂ input increases the inventory of inert solids and drastically reduces the average activity of the sorbent. In fact, the actual effective maximum average conversion of the particles takes on a value similar to that of the residual conversion of lime, even in the presence of the make-up flow. The sharp decrease in sorbent activity assumed for this scenario is the result of the direct effect of X_{sulf} subtracting net points of X_{ave} (Eq. (6)). This can be considered as a too conservative assumption, because CaSO₄ has been shown to be able to react not only with the active CaO for CO₂ capture but also with the non-active lime fraction [25]. However, in Configuration 2, when the flue gas is desulfurized in the CFB reactor prior to entering the CO₂ capture system, the E_{carb} increases up to 80% for the same operating conditions due mainly to the higher $X_{ave,e}$. If the sorbent is subjected to a process to increase its average activity (Configuration 3), a CO₂ capture efficiency of 93% can be attained under the favorable conditions of this configuration.

In the case of the solids streams, it can be seen from Configurations 2 and 3 that the ash and CaSO₄ contents in the partially carbonated and calcined solids streams are similar (see Table 4), although they are slightly higher in the latter case because more coal is fed to the calciner in order to calcine the higher flow of CaCO₃ formed in the carbonator. On the other hand, the amount of CaSO₄ formed when using Configuration 1 is significantly higher (around 15%).

It is already clear from solving solutions of the reference configurations that the CO₂ capture process can achieve a low performance due to the reduction of sorbent activity and the accumulation of inerts in the system. In order to improve its performance (increase the activity of the sorbent and purge the inerts), the main process variable that needs to be adjusted is the make-up flow of fresh limestone. This section analyzes how the F_0/F_{CO_2} ratio affects the CO₂ capture efficiency and the concentration of inerts, and the differences between each configuration. The procedure and the input variables used are the same as in the reference scenarios. The calculated CO₂ capture efficiencies are depicted in Fig. 3, whereas Figs. 5a and 5b show the weight percentage of ashes and CaSO₄ respectively in the stream of the partially carbonated solids that is transported from the carbonator to the calciner.

As can be seen in Fig. 3, for low values of F_0/F_{CO_2} , the higher the make-up flow, the higher the CO₂ capture efficiency due to the improvement of the effective maximum average conversion of the sorbent (depicted in Fig. 4) and the rise of the circulation rates of calcium between reactors as the inert solids concentration decreases. The rate at which the E_{carb} increases as a function of the F_0/F_{CO_2} ratio is different for each configuration. As mentioned in the previous section, these differences can be explained on the basis of the composition of the inventory of solids in the system and the effective maximum average conversion of the particles (see Fig. 4), which is reduced due to the presence of a larger amount of SO₂ in Configuration 1, and increased in Configuration 3 by the reactivation stage. It is also clear from Fig. 3 that after a certain value of F_0/F_{CO_2} is reached (0.19, 0.14 and 0.07 for Configurations 1, 2

Table 3
Molar flows and compositions of the gas streams of Fig. 1.

Configuration	Composition	Gas streams				
		Flue gas (1)	Flue gas “without” CO ₂ (2)	CO ₂ recycle (6)	Concentrated CO ₂ (9)	Concentrated CO ₂ (11)
1	Molar flow (kmol/s)	13.3	12.3	8.3	10.1	4.1
	CO ₂ (%v)	15.3	8.3	56.1	77.6	77.6
	SO ₂ (ppm)	844	91	37	52	52
2	Molar flow (kmol/s)	13.3	11.6	9.7	12.2	5.1
	CO ₂ (%v)	15.3	3.5	57.3	79.2	79.2
	SO ₂ (ppm)	84	10	36	49	49
3	Molar flow (kmol/s)	13.3	11.4	10.5	13.2	5.7
	CO ₂ (%v)	15.3	1.2	57.6	79.6	79.6
	SO ₂ (ppm)	84	10	35	49	49

Table 4
Mass flows and compositions of the solids streams of Fig. 1.

Configuration	Composition	Solids streams				
		Partially carbonated solids (3)	Coal (4)	Fresh limestone (7)	Purge (8)	Calcined solids (10)
1	Mass flow (kg/s)	1005.6	31.3	20.3	13.3	959.9
	CaCO ₃ (%w)	10.2	–	100	–	–
	CaO (%w)	69.7	–	–	79.1	79.1
	Ash (%w)	5.6	–	–	5.9	5.9
	CaSO ₄ (%w)	14.5	–	–	15.0	15.0
2	Mass flow (kg/s)	1004.5	36.4	20.3	12.8	932.7
	CaCO ₃ (%w)	16.2	–	100	–	–
	CaO (%w)	70.8	–	–	86.1	86.1
	Ash (%w)	6.6	–	–	7.1	7.1
	CaSO ₄ (%w)	6.4	–	–	6.8	6.8
3	Mass flow (kg/s)	1004.5	39.0	20.3	12.9	920.9
	CaCO ₃ (%w)	18.8	–	100	–	–
	CaO (%w)	67.6	–	–	85.2	85.2
	Ash (%w)	7.0	–	–	7.6	7.6
	CaSO ₄ (%w)	6.6	–	–	7.2	7.2

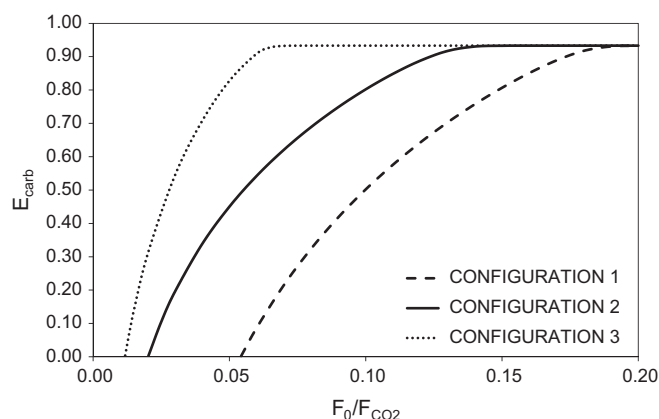


Fig. 3. Evolution of the CO₂ capture efficiency with the F_0/F_{CO_2} ratio.

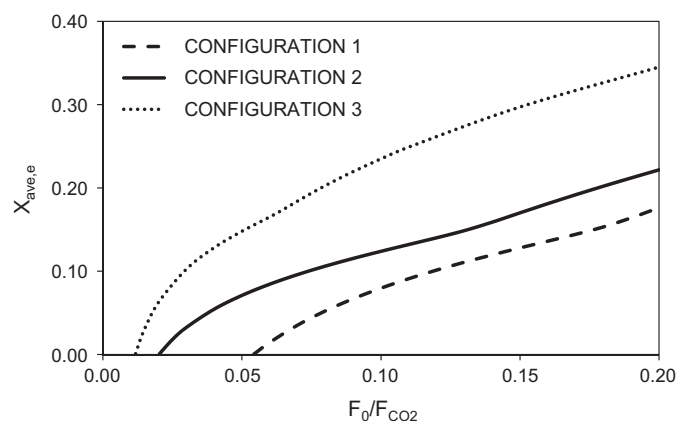


Fig. 4. Evolution of $X_{ave,e}$ with the F_0/F_{CO_2} ratio for the different configurations.

and 3 respectively) the activity of the sorbent is no longer a limiting factor and CO₂ capture efficiencies are close to the maximum allowed by the equilibrium.

As it can be seen in Fig. 5a, the ash content in the system (X_{ash}) rises sharply as the F_0/F_{CO_2} ratio approaches to zero. As shown above, for low F_0/F_{CO_2} ratios the differences observed in the ash content are mainly due to changes in the coal requirements in the calciner, since different amounts of CO₂ are captured in each configuration, thus modifying the heat demand in the calciner. When the make-up flow increases the CO₂ capture efficiencies reach values close to equilibrium, and there are almost no differences in the ash content. The mass fraction of CaSO₄ in the

carbonator (Fig. 5b), X_{CaSO_4} , follows the same trend as the ashes when comparing Configurations 2 and 3, because the input of SO₂ into the system is mainly due to the sulfur in the coal fed into the calciner. However, Configuration 1 shows significantly higher X_{CaSO_4} values, since there is an additional input of sulfur to the CaL system from the flue gas.

It can be inferred from the previous results that the main impact on CaL performance is the input of sulfur into the system. In order to compare the deactivating effect of sulfur to that caused by the accumulation of inerts, a series of calculations were carried out. It was found that when the sulfur content of the coal burnt in the calciner was increased from 0.5% (reference case) to 1% (73.5%

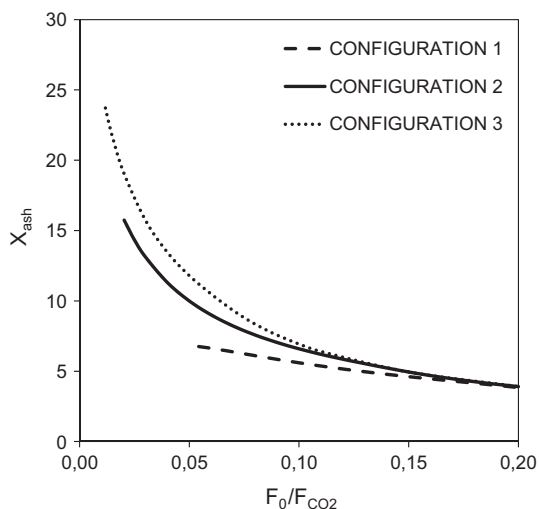


Fig. 5a. Mass fraction of ashes in stream (3).

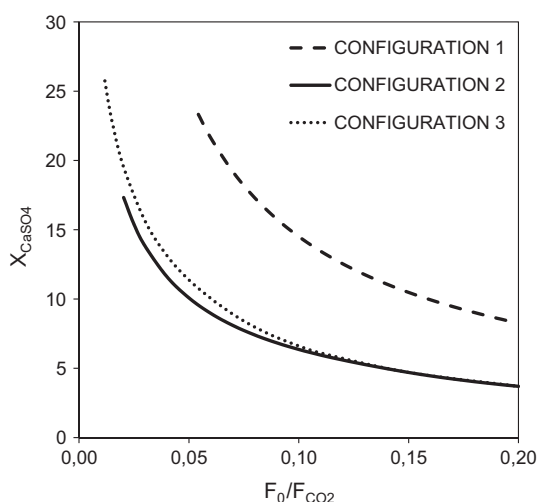


Fig. 5b. Mass fraction of CaSO_4 in stream (3).

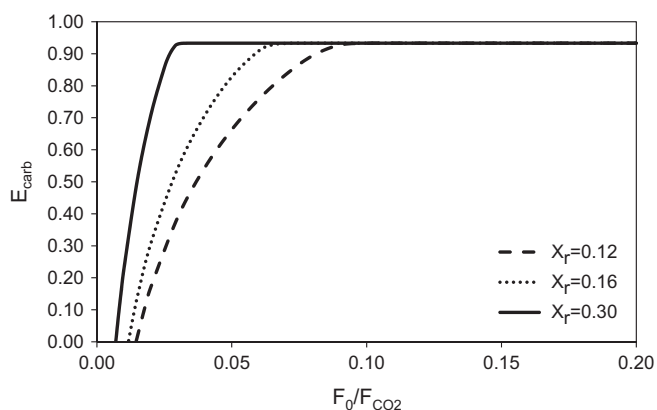


Fig. 6. Evolution of the CO_2 capture efficiency with the F_0/F_{CO_2} ratio for different extents of reactivation in Configuration 3.

C, 4.0% H, 1.0% S, 8.0% O, 8.0% H_2O , 0.5% N, 5.0% Ash (LHV: 30.0 MJ/kg)) the F_0/F_{CO_2} ratios required to maintain a CO_2 capture efficiency equal to 90% were 0.20, 0.15 and 0.08 for Configurations 1, 2 and 3

respectively. These values are similar to those required when using a coal with a sulfur content equal to that of the reference case with 20% ashes (58.0% C, 4.0% H, 0.5% S, 8.0% O, 8.0% H_2O , 1.5% N, 20.0% Ash (LHV: 24.5 MJ/kg)). Therefore, in these specific conditions, an increase in the coal sulfur content of 0.5% with respect to the reference coal has a similar effect to a rise of 15% in the ash percentage. However, it should be noted that the specific values can change as a function of the definition of the coal composition.

Finally, Fig. 6 summarizes the impact of different sorbent qualities on the E_{carb} for different make up flows of sorbent. In general CaL technology pursues high CO_2 capture efficiencies while minimizing the make-up flow of sorbent. Unless there is a strong synergy with a cement producer (which would also impose limits on the composition of the purge material used), low limestone consumption is always an economic advantage [46,47]. F_0 can be reduced when using high-quality coals and/or when the sorbent is reactivated. The effect of the reactivation was analyzed for a system which follows the scheme of Configuration 3, where lime has residual conversions of 0.12, 0.16 (reference case of Configuration 3) and 0.30. In these cases, a 90% CO_2 capture efficiency is attained when the F_0/F_{CO_2} ratio is 0.08, 0.06 and 0.03 respectively. Furthermore, the CO_2 capture efficiency was analyzed as a function of the F_0/F_{CO_2} ratio, as depicted in Fig. 6. It can be seen that the CO_2 capture efficiency approaches zero for low F_0/F_{CO_2} ratios, and these limiting ratios are lower when the extent of reactivation increases. However, it will always be necessary to feed a certain make-up flow of fresh limestone to attain reasonable CO_2 capture efficiencies, although the make-up flow can be reduced as a function of the reactivation level achieved by the sorbent.

4. Conclusion

CaL facilities for postcombustion CO_2 capture have a continuous input of ashes and SO_2 that depends on the flue gas desulfurization level in the reference plant and on the coal fed into the calciner. The increase in the feed of ashes and SO_2 to the system leads to a lower CO_2 capture efficiency due to the sulfation of the active CaO and a reduction in the inventory of active CaO in the carbonator. The results obtained in this work indicate that the main impact on CaL performance is caused principally by the input of sulfur into the system. With low sulfur coals (1% S in the boiler and 0.5% in the calciner) the introduction of a modest reactivation step ($X_r = 0.16$) reduces the make-up flow required to attain an $E_{\text{carb}} = 0.9$ of around 50%. However, even with an effective reactivating step leading to a lime residual conversion equal to 0.30, there is a need for a minimum make-up flow of limestone of about 0.03 (F_0/F_{CO_2}) to avoid the effects of the inerts.

The analysis carried out in this work confirms that when operating with low make-up flows, the carbonator efficiency shows high sensitivity to the composition of the coal of the calciner and the SO_2 content in the flue gas. The methodology proposed in this study seems to be a valuable tool for quantitatively selecting make-up flows for different configurations and different coal qualities.

Acknowledgments

M.E. Diego acknowledges a fellowship Grant under the CSIC JAE Programme, co-funded by the European Social Fund. The financial support given by the RECaL project (RCFR-2012-RECaL) is also acknowledged.

References

- [1] Metz B, Davidson O, Coninck H, Loos M, Meyer L. Special report on carbon dioxide capture and storage. Intergovernmental panel on climate change. Cambridge, UK: Cambridge University Press; 2005.

- [2] Rodríguez N, Alonso M, Abanades JC. Experimental investigation of a circulating fluidized-bed reactor to capture CO₂ with CaO. *AIChE J* 2011;57:1356–66.
- [3] Charitos A, Rodríguez N, Hawthorne C, Alonso M, Zieba M, Arias B, et al. Experimental validation of the calcium looping CO₂ capture process with two circulating fluidized bed carbonator reactors. *Ind Eng Chem Res* 2011;50:9685–95.
- [4] Sánchez-Biezma A, Ballesteros JC, Díaz L, de Zárraga E, Álvarez FJ, López J, et al. Postcombustion CO₂ capture with CaO. Status of the technology and next steps towards large scale demonstration. *Energy Procedia* 2011;4:852–9.
- [5] Sánchez-Biezma A, Díaz L, López J, Arias B, Paniagua J, de Zárraga E, Álvarez J, Abanades JC. La Pereda CO₂: a 1.7 MW Pilot to test post-combustion CO₂ capture with CaO. In: 21st International conference on fluidized bed combustion, Naples (Italy); 2012, p. 365–72.
- [6] Hawthorne C, Dieter H, Bidwe A, Schuster A, Scheffknecht G, Unterberger S, et al. CO₂ capture with CaO in a 200 kW_{th} dual fluidized bed pilot plant. *Energy Procedia* 2011;4:441–8.
- [7] Dieter H, Hawthorne C, Bidwe AR, Zieba M, Scheffknecht G. The 200 kW_{th} dual fluidized bed calcium looping pilot plant for efficient CO₂ capture: plant operating experiences and results. In: 21st International conference on fluidized bed combustion, Naples (Italy); 2012, p. 397–404.
- [8] Galloy A, Ströhle J, Epple B. Design and operation of a 1 MW_{th} carbonate and chemical looping CCS test rig. *VGB Power Tech* 2011;91:64–8.
- [9] Plötz S, Bayrak A, Galloy A, Kremer J, Orth M, Wiecezorek M, Ströhle J, Epple B. First carbonate looping experiments with a 1 MW_{th} test facility consisting of two interconnected CFBs. In: 21st International conference on fluidized bed combustion, Naples (Italy); 2012, p. 421–8.
- [10] Shimizu T, Hiramata T, Hosoda H, Kitano K, Inagaki M, Tejima K. A twin fluid-bed reactor for removal of CO₂ from combustion processes. *Chem Eng Res Des* 1999;77:62–8.
- [11] Rodríguez N, Alonso M, Grasa G, Abanades JC. Heat requirements in a calciner of CaCO₃ integrated in a CO₂ capture system using CaO. *Chem Eng J* 2008;138:148–54.
- [12] Abanades JC, Anthony EJ, Wang J, Oakey JE. Fluidized bed combustion systems integrating CO₂ capture with CaO. *Environ Sci Technol* 2005;39:2861–6.
- [13] Romeo LM, Abanades JC, Escosa JM, Paño J, Giménez A, Sánchez-Biezma A, et al. Oxyfuel carbonation/calcination cycle for low cost CO₂ capture in existing power plants. *Energy Convers Manage* 2008;49:2809–14.
- [14] Romano M. Coal-fired power plant with calcium oxide carbonation for postcombustion CO₂ capture. *Energy Procedia* 2009;1:1099–106.
- [15] Hawthorne C, Trossmann M, Galindo Cifre P, Schuster A, Scheffknecht G. Simulation of the carbonate looping power cycle. *Energy Procedia* 2009;1:1387–94.
- [16] Yongping Y, Rongrong Z, Liqiang D, Kavosh M, Patchigolla K, Oakey J. Integration and evaluation of a power plant with a CaO-based CO₂ capture system. *Int J Greenhouse Gas Control* 2010;4:603–12.
- [17] Lasheras A, Ströhle J, Galloy A, Epple B. Carbonate looping process simulation using a 1D fluidized bed model for the carbonator. *Int J Greenhouse Gas Control* 2011;5:686–93.
- [18] Martínez I, Murillo R, Grasa G, Abanades JC. Integration of a Ca looping system for CO₂ capture in existing power plants. *AIChE J* 2011;57:2599–607.
- [19] Lisbona P, Martínez A, Lara Y, Romeo LM. Integration of carbonate CO₂ capture cycle and coal-fired power plants. A comparative study for different sorbents. *Energy Fuels* 2010;24:728–36.
- [20] Romeo LM, Lara Y, Lisbona P, Escosa JM. Optimizing make-up flow in a CO₂ capture system using CaO. *Chem Eng J* 2009;147:252–8.
- [21] Li Z-s, Cai N-s, Croiset E. Process analysis of CO₂ capture from flue gas using carbonation/calcination cycles. *AIChE J* 2008;54:1912–25.
- [22] Li Y, Buchi S, Grace JR, Lim CJ. SO₂ removal and CO₂ capture by limestone resulting from calcination/sulfation/carbonation cycles. *Energy Fuels* 2005;19:1927–34.
- [23] Sun P, Grace JR, Lim CJ, Anthony EJ. Removal of CO₂ by calcium-based sorbents in the presence of SO₂. *Energy Fuels* 2006;21:163–70.
- [24] Ryu H-J, Grace JR, Lim CJ. Simultaneous CO₂/SO₂ capture characteristics of three limestones in a fluidized-bed reactor. *Energy Fuels* 2006;20:1621–8.
- [25] Grasa GS, Alonso M, Abanades JC. Sulfation of CaO particles in a carbonation/calcination loop to capture CO₂. *Ind Eng Chem Res* 2008;47:1630–5.
- [26] Manovic V, Anthony EJ. Sequential SO₂/CO₂ capture enhanced by steam reactivation of a CaO-based sorbent. *Fuel* 2008;87:1564–73.
- [27] Hughes RW, Lu D, Anthony EJ, Wu Y. Improved long-term conversion of limestone-derived sorbents for in situ capture of CO₂ in a fluidized bed combustor. *Ind Eng Chem Res* 2004;43:5529–39.
- [28] Manovic V, Anthony EJ. Steam reactivation of spent CaO-based sorbent for multiple CO₂ capture cycles. *Environ Sci Technol* 2007;41:1420–5.
- [29] Fennell PS, Davidson JF, Dennis JS, Hayhurst AN. Regeneration of sintered limestones sorbents for the sequestration of CO₂ from combustion and other systems. *J Energy Inst* 2007;80:116–9.
- [30] Manovic V, Lu D, Anthony EJ. Steam hydration of sorbents from a dual fluidized bed CO₂ looping cycle reactor. *Fuel* 2008;87:3344–52.
- [31] Grasa G, Murillo R, Alonso M, González B, Rodríguez N, Abanades JC. Steam reactivation of CaO-based natural sorbents applied to a carbonation/calcination loop for CO₂ capture. In: 4th International conference on clean coal technologies, Dresden, Germany; 2009.
- [32] Arias B, Grasa GS, Abanades JC. Effect of sorbent hydration on the average activity of CaO in a Ca-looping system. *Chem Eng J* 2010;163:324–30.
- [33] Materic BV, Sheppard C, Smedley SI. Effect of repeated steam hydration reactivation on CaO-based sorbents for CO₂ capture. *Environ Sci Technol* 2010;44:9496–501.
- [34] Phalak N, Deshpande N, Fan LS. Investigation of high-temperature steam hydration of naturally derived calcium oxide for improved carbon dioxide capture capacity over multiple cycles. *Energy Fuels* 2012;26:3903–9.
- [35] Arias B, Grasa GS, Alonso M, Abanades JC. Post-combustion calcium looping process with a highly stable sorbent activity by recarbonation. *Energy Environ Sci* 2012;5:7353–9.
- [36] Alonso M, Rodríguez N, Grasa G, Abanades JC. Modelling of a fluidized bed carbonator reactor to capture CO₂ from a combustion flue gas. *Chem Eng Sci* 2009;64:883–91.
- [37] Rodríguez N, Alonso M, Abanades JC. Average activity of CaO particles in a calcium looping system. *Chem Eng J* 2010;156:388–94.
- [38] Charitos A, Hawthorne C, Bidwe AR, Korovesis L, Schuster A, Scheffknecht G. Hydrodynamic analysis of a 10 kW_{th} calcium looping dual fluidized bed for post-combustion CO₂ capture. *Powder Technol* 2010;200:117–27.
- [39] Diego ME, Arias B, Abanades JC. Modeling the solids circulation rates and solids inventories of an interconnected circulating fluidized bed reactor system for CO₂ capture by calcium looping. *Chem Eng J* 2012;198–199:228–35.
- [40] Coppola A, Montagnaro F, Salatino P, Scala F. Attrition of limestone during fluidized bed calcium looping cycles for CO₂ capture. *Combust Sci Technol* 2012;184:929–41.
- [41] Grasa GS, Abanades JC. CO₂ capture capacity of CaO in long series of carbonation/calcination cycles. *Ind Eng Chem Res* 2006;45:8846–51.
- [42] Blamey J, Anthony EJ, Wang J, Fennell PS. The calcium looping cycle for large-scale CO₂ capture. *Prog Energy Combust Sci* 2010;36:260–79.
- [43] Yu F-C, Phalak N, Sun Z, Fan L-S. Activation strategies for calcium-based sorbents for CO₂ capture: a perspective. *Ind Eng Chem Res* 2011;51:2133–42.
- [44] Donat F, Florin NH, Anthony EJ, Fennell PS. Influence of high-temperature steam on the reactivity of CaO sorbent for CO₂ capture. *Environ Sci Technol* 2012;46:1262–9.
- [45] Arias B, Grasa G, Abanades JC, Manovic V, Anthony EJ. The effect of steam on the fast carbonation reaction rates of CaO. *Ind Eng Chem Res* 2012;51:2478–82.
- [46] Dean CC, Blamey J, Florin NH, Al-Jeboori MJ, Fennell PS. The calcium looping cycle for CO₂ capture from power generation, cement manufacture and hydrogen production. *Chem Eng Res Des* 2011;89:836–55.
- [47] Romeo LM, Catalina D, Lisbona P, Lara Y, Martínez A. Reduction of greenhouse gas emissions by integration of cement plants, power plants, and CO₂ capture systems. *Greenhouse Gas Sci Technol* 2011;1:72–82.